

A Linux PC cluster for lattice QCD with exact chiral symmetry

Ting-Wai Chiu, Tung-Han Hsieh, Chao-Hsi Huang, Tsung-Ren Huang

Department of Physics, National Taiwan University
Taipei, Taiwan 106, Taiwan.
E-mail: twchiu@phys.ntu.edu.tw

Abstract

A computational system for lattice QCD with exact chiral symmetry is described. The platform is a home-made Linux PC cluster, built with off-the-shelf components. At present the system constitutes of 64 nodes, with each node consisting of one Pentium 4 processor (1.6/2.0/2.5 GHz), one Gbyte of PC800/1066 RDRAM, one 40/80/120 Gbyte hard disk, and a network card. The computationally intensive parts of our program are written in SSE2 codes. The speed of our system is estimated to be 70 Gflops, and its price/performance ratio is better than \$1.0/Mflops for 64-bit (double precision) computations in quenched QCD. We discuss how to optimize its hardware and software for computing quark propagators via the overlap Dirac operator.

PACS numbers: 11.15.Ha, 11.30.Rd, 12.38.Gc

Keywords: Lattice QCD, Overlap Dirac operator, Linux PC cluster

1 Introduction

Our objective is to extract physics from lattice QCD with possibly minimal amount of computations. Obviously, the required computing power exceeds that of any desktop personal computer currently available in the market. Thus, for one without supercomputer resources, building a computational system [1] seems to be inevitable if one really wishes to pursue a meaningful number of any physical quantity from lattice QCD. However, the feasibility of such a project depends not only on the funding, but also on the theoretical advancement of the subject, namely, the realization of exact chiral symmetry on the lattice [2, 3]. Now, if we also take into account of the current price/performance of PC hardware components (CPU + RAM + hard disk¹), it seems to be the right time to rejuvenate the project [1] with a new goal - to build a computational system for lattice QCD with exact chiral symmetry. In this paper, we outline the essential features of a Linux PC cluster (64 nodes) which has been built at National Taiwan University. In particular, we discuss how to optimize its hardware and software for lattice QCD with overlap Dirac operator.

First, we start from quenched QCD calculations (i.e., ignoring any internal quark loops by setting $\det D = 1$). Thus, our first task is to compute quark propagators in the gluon field background, for a sequence of configurations generated stochastically with weight $\exp(-\mathcal{A}_g)$ (\mathcal{A}_g : pure gluon action). Then the hadronic observables such as meson and baryon correlation functions can be constructed, and from which the hadron masses and decay constants can be extracted. We use the Creutz-Cabbibo-Marinari heat bath algorithm [4, 5] to generate ensembles of $SU(3)$ gauge configurations.

The computation of quark propagators depends on the scheme of lattice fermions, the hard core of lattice QCD. In general, one requires that any quark propagator coupling to physical hadrons must be of the form [6]

$$(D_c + m_q)^{-1} , \quad (1)$$

where m_q is the bare quark mass, and D_c is a chirally symmetric and anti-hermitian Dirac operator [$D_c\gamma_5 + \gamma_5 D_c = 0$ and $(iD_c)^\dagger = iD_c$]. Here we assume that D_c is doubler-free, has correct continuum behavior, and $D = D_c(1 + raD_c)^{-1}$ is exponentially local for smooth gauge backgrounds. Note that the way m_q coupling to D_c is the same as that in the continuum. The chiral symmetry of D_c (even at finite lattice spacing) is the crucial feature of any quark coupling to physical hadrons. Otherwise, one could hardly reproduce the low energy strong interaction phenomenology from lattice QCD.

For any massless lattice Dirac operator D satisfying the Ginsparg-Wilson relation [7]

$$D\gamma_5 + \gamma_5 D = 2raD\gamma_5 D , \quad (2)$$

it can be written as [8]

$$D = D_c(1 + raD_c)^{-1} ,$$

and the bare quark mass is naturally added to the D_c in the numerator [6],

$$D(m_q) = (D_c + m_q)(1 + raD_c)^{-1} .$$

¹The emergence of low-price and high-capacity (> 100 Gbyte) IDE hard disk turns out to be also rather crucial for this project, since the data storage is enormous.

Then the quenched quark propagator becomes

$$(D_c + m_q)^{-1} = (1 - rm_q a)^{-1} [D(m_q)^{-1} - ra] \quad (3)$$

If we fix one of the end points at $(\vec{0}, 0)$ and use the Hermiticity $D^\dagger = \gamma_5 D \gamma_5$, then only 12 (3 colors times 4 Dirac indices) columns of

$$D(m_q)^{-1} = D^\dagger(m_q) \{D(m_q) D^\dagger(m_q)\}^{-1} \quad (4)$$

are needed for computing the time correlation functions of hadrons. Now our problem is how to optimize a PC cluster to compute $D(m_q)^{-1}$ for a set of bare quark masses.

The outline of this paper is as follows. In Section 2, we briefly review our scheme of computing quark propagators via the overlap Dirac operator. The details have been given in Ref. [9]. In Section 3, we discuss a simple scheme of memory management for the nested conjugate gradient loops. In Section 4, we discuss how to implement the SSE2 codes for the computationally intense parts of our program. In Section 5, the performance of our system is measured in terms of a number of tests pertaining to the computation of quark propagators. In Section 6, we conclude with some remarks and outlooks.

2 Computational Scheme for quark propagators

The massless overlap Dirac operator [3] reads as

$$D = m_0 a^{-1} \left(\mathbb{1} + \gamma_5 \frac{H_w}{\sqrt{H_w^2}} \right) \quad (5)$$

where H_w denotes the Hermitian Wilson-Dirac operator with a negative parameter $-m_0$,

$$H_w = \gamma_5 D_w = \gamma_5 (-m_0 + \gamma_\mu t_\mu + W) , \quad (6)$$

$\gamma_\mu t_\mu$ the naive fermion operator, and W the Wilson term. Then D (5) satisfies the Ginsparg-Wilson relation (2) with $r = 1/(2m_0)$. In this paper, we always fix $m_0 = 1.3$ for our computations. Details of our implementation have been given in Ref. [9].

Basically, we need to solve the following linear system

$$\begin{aligned} & D(m_q) D^\dagger(m_q) Y \\ &= \left\{ m_q^2 + \left(2m_0^2 - \frac{m_q^2}{2} \right) \left[1 + \frac{(\gamma_5 \pm 1)}{2} H_w \frac{1}{\sqrt{H_w^2}} \right] \right\} Y = \mathbb{1} \end{aligned} \quad (7)$$

by conjugate gradient (CG). Then the quark propagators can be obtained through (4). With Zolotarev optimal rational approximation [10, 11, 12, 13] to $(H_w^2)^{-1/2}$, the multiplication²

$$\begin{aligned} & H_w \left(\frac{1}{\sqrt{H_w^2}} \right) Y, \quad h_w \equiv \frac{H_w}{\lambda_{min}} \\ & \simeq h_w (h_w^2 + c_{2n}) \sum_{l=1}^n \frac{b_l}{h_w^2 + c_{2l-1}} Y = h_w (h_w^2 + c_{2n}) \sum_{l=1}^n b_l Z_l \end{aligned} \quad (8)$$

²Note that the Zolotarev optimal rational polynomial in Eq. (8) is in the form $r^{(n,n)}$ which is different from $r^{(n-1,n)}$ used in Ref. [9]. We refer to Ref. [13] for further discussions.

can be evaluated by invoking another conjugate gradient process to the linear systems

$$(h_w^2 + c_{2l-1})Z_l = Y, \quad l = 1, \dots, n. \quad (9)$$

where

$$\begin{aligned} c_l &= \frac{\operatorname{sn}^2\left(\frac{lK'}{2n+1}; \kappa'\right)}{1 - \operatorname{sn}^2\left(\frac{lK'}{2n+1}; \kappa'\right)} \\ b_l &= d_0 \frac{\prod_{i=1}^{n-1} (c_{2i} - c_{2l-1})}{\prod_{i=1, i \neq l}^n (c_{2i-1} - c_{2l-1})} \\ d_0 &= \frac{2\lambda}{1 + \lambda} \prod_{l=1}^n \frac{1 + c_{2l-1}}{1 + c_{2l}} \\ \lambda &= \prod_{l=1}^{2n+1} \frac{\Theta^2\left(\frac{2lK'}{2n+1}; \kappa'\right)}{\Theta^2\left(\frac{(2l-1)K'}{2n+1}; \kappa'\right)}. \end{aligned}$$

Here Θ denotes the elliptic theta function, and the Jacobian elliptic function $\operatorname{sn}(u; \kappa')$ is defined by the elliptic integral

$$u = \int_0^{\operatorname{sn}} \frac{dt}{\sqrt{(1-t^2)(1-\kappa'^2 t^2)}},$$

and K' is the complete elliptic integral of the first kind with modulus κ' ,

$$K' = \int_0^1 \frac{dt}{\sqrt{(1-t^2)(1-\kappa'^2 t^2)}},$$

where $\kappa' = \sqrt{1 - 1/b}$, $b = \lambda_{max}^2 / \lambda_{min}^2$, and λ_{max}^2 and λ_{min}^2 are the maximum and the minimum of the eigenvalues of H_w^2 .

Instead of solving each Z_l individually, one can use multi-shift CG algorithm [14, 15], and obtain all Z_l altogether, with only a small fraction of the total time what one had computed each Z_l separately. Evidently, one can also apply multi-shift CG algorithm to (7) to obtain several quark propagators with different bare quark masses.

In order to improve the accuracy of the rational approximation as well as to reduce the number of iterations in the inner CG loop, it is *crucial* to narrow the interval $[1, b]$ by projecting out the largest and some low-lying eigenmodes of H_w^2 . We use Arnoldi algorithm [16] to project these eigenmodes. Denoting these eigenmodes by

$$H_w u_j = \lambda_j u_j, \quad j = 1, \dots, k, \quad (10)$$

then we project the linear systems (9) to the complement of the vector space spanned by these eigenmodes

$$(h_w^2 + c_{2l-1})\bar{Z}_l = \bar{Y} \equiv \left(1 - \sum_{j=1}^k u_j u_j^\dagger\right) Y, \quad l = 1, \dots, n. \quad (11)$$

In the set of projected eigenvalues of H_w^2 , $\{\lambda_j^2, j = 1, \dots, k\}$, we use λ_{max}^2 and λ_{min}^2 to denote the least upper bound and the greatest lower bound of the eigenvalues of \bar{H}_w^2 , where

$$\bar{H}_w = H_w - \sum_{j=1}^k \lambda_j u_j u_j^\dagger.$$

Then the eigenvalues of

$$h_w^2 = \bar{H}_w^2 / \lambda_{min}^2$$

fall into the interval $(1, b)$, $b = \lambda_{max}^2 / \lambda_{min}^2$.

Now the matrix-vector multiplication (8) can be expressed in terms of the projected eigenmodes (10) plus the solution obtained from the conjugate gradient loop (11) in the complementary vector space, i.e.,

$$H_w \frac{1}{\sqrt{H_w^2}} Y \simeq \frac{1}{\lambda_{min}} H_w (h_w^2 + c_{2n}) \sum_{l=1}^n b_l \bar{Z}_l + \sum_{j=1}^k \frac{\lambda_j}{\sqrt{\lambda_j^2}} u_j u_j^\dagger Y \equiv S \quad (12)$$

Then the breaking of exact chiral symmetry (2) can be measured in terms of

$$\sigma = \frac{|S^\dagger S - Y^\dagger Y|}{Y^\dagger Y}. \quad (13)$$

In practice, one has no difficulties to attain $\sigma < 10^{-12}$ for most gauge configurations on a finite lattice [13].

Now the computation of quark propagators involves two nested conjugate gradient loops: the so-called inner CG loop (11), and the outer CG loop (7). The inner CG loop is the price what one pays for preserving the exact chiral symmetry at finite lattice spacing.

3 Memory management

In this section we discuss how to configure the hardware and software of a PC cluster such that it can attain the optimal price/performance for the execution of the nested CG loops, (7) and (11).

First, we examine how much memory is required for computing one of the 12 columns of the quark propagators for a set of bare quark masses, since each column can be computed independently. If the required memory can be allocated in a single node, then each node can be assigned to work on one of the 12 columns of the quark propagators. Then the maximum speed of a PC cluster is attained since there is no communication overheads. Nevertheless, the memory (RDRAM) is the most expensive component, thus its amount should be minimized even though the maximum memory at each node can be up to 4 Gbyte. On the other hand, if one distributes the components of the nested CG loops across the nodes and performs parallel computations (with MPI) through a fast network switch, then the memory at each node can be minimal. However, the cost of a fast network switch and its accessories is rather expensive, and also the efficiency of the entire system will be greatly reduced due to the communication overheads. Therefore, to optimize the price/performance of the PC cluster relies on what is the minimal memory required for computing one of the 12 columns of the quark propagators.

Let $N_s = L^3 \times T$ denote the total number of lattice sites, then each column of D^{-1} with double complex (16 bytes) entries takes

$$N_v = N_s \times 12 \times 16 \text{ bytes.} \quad (14)$$

Using N_v or one column as the unit, we list the memory space of all components during the execution of the nested CG loops :

- Gauge links: 3.
- Number of projected low-lying eigenmodes: k
- Quark propagators [i.e., Y in (7)] of N_m masses: $N_m/2$.
(Note that each Y only takes 1/2 column since it is chiral.)
- Conjugate gradient vectors in the CG algorithm: $N_m/2$.
- Residual vector for the outer CG loop: 1/2.
- The vector \bar{Y}_1 (of the smallest bare quark mass) at the interface between the inner and the outer CG loops: 1.
- The inner CG loop: $2n + 3$ (where n is the degree of Zolotarev rational polynomial), which consists of
 - (i) $\{Z_l\}$ vectors: n ;
 - (ii) Conjugate gradient vectors $\{w_l\}$: n ;
 - (iii) Residual vector (r): 1;
 - (iv) $H_w |w_1\rangle$: 1;
 - (v) $H_w^2 |w_1\rangle$: 1.

Therefore, the memory space for all components of the nested CG loops is

$$N_{cg} = (N_m + 1/2) + (2n + 3) + k + 3 = N_m + 2n + k + 6.5 \text{ (columns)} \quad (15)$$

A schematic diagram of all components of the nested CG loops is sketched in Fig. 1.

Suppose we wish to compute quark propagators on the $16^3 \times 32$ lattice (at $\beta = 6.0$), with parameters $k = 16$, $n = 16$, and $N_m = 16$. Then, according to (14) and (15),

$$\begin{aligned} N_v &\simeq 0.024 \text{ Gbyte ,} \\ N_{cg} &= 70.5 \text{ columns ,} \end{aligned}$$

the required memory for all components of the nested CG loops is

$$N_{cg} \times N_v \simeq 70.5 \times 0.024 = 1.7 \text{ Gbyte}$$

This seems to imply that one should install³ four stripes of 512 Mbyte modules (i.e. total 2 Gbyte) at each node, if one wishes to let each node compute independently, and to attain the maximum speed of the PC cluster. However, this is a rather expensive solution at this

³At present, most Pentium 4 motherboards designed for housing PC800 RDRAM have 4 memory slots.

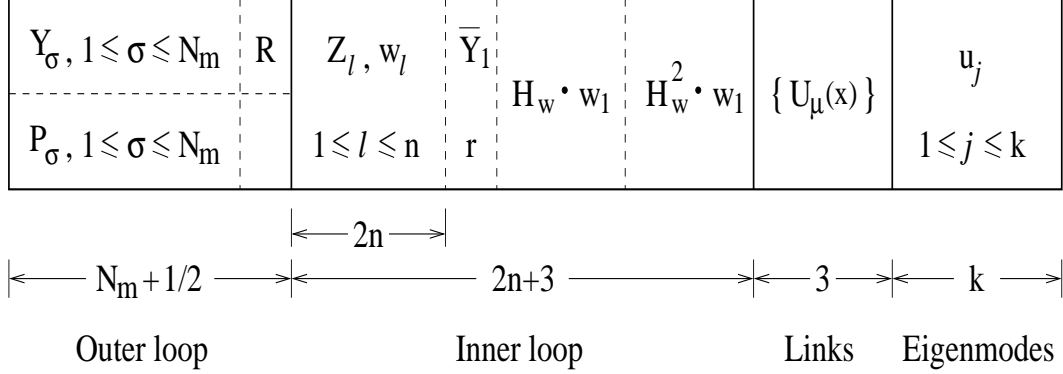


Figure 1: A schematic diagram of all memory allocations for the nested CG loops.

moment, in view of the current price of 512 Mbyte modules. On the other hand, if one distributes the components of the nested CG loops across the nodes and performs parallel computations (with MPI) through a fast network switch, then the price/performance seems to be even worse than the former solution.

Fortunately, we observe that *not* all column vectors are used simultaneously at any step of the nested CG loops, and also the computationally intense part is at the inner CG loop. Thus we can use the hard disk as the virtual memory for the storage of the intermediate solution vectors and their conjugate gradient vectors ($Y_\sigma, P_\sigma, \sigma = 1, \dots, N_m$) at each iteration of the outer CG loop, while the CPU is working on the inner CG loop. Then the minimal physical memory required at each node can be greatly reduced. Also, the projected eigenmodes are not required to be kept inside the memory, since they are only needed at the start of the inner CG loop to compute \bar{Y}_1 (for the smallest bare quark mass),

$$\bar{Y}_1 \equiv \left(1 - \sum_{j=1}^k u_j u_j^\dagger\right) Y_1,$$

and

$$\sum_{j=1}^k \frac{\lambda_j}{\sqrt{\lambda_j^2}} u_j u_j^\dagger Y_1 \equiv \varepsilon_p Y_1$$

where $\varepsilon_p Y_1$ is only needed for computing S (12) at the completion of the inner CG loop. Thus one has the options to keep the vector $\varepsilon_p Y_1$ inside the memory during the entire inner CG loop or save it to the hard disk and then retrieve it at the completion of the inner CG loop. Further, since \bar{Y}_1 is only needed at the start of the inner CG loop, so it can share the same memory location with the residual vector r .

Now it is clear that the minimum memory at each node (without suffering a substantial loss in the performance) is

$$N_{cg}^{min} = (2n + 3) + 3 = 2n + 6 \text{ (columns)},$$

which suffices to accommodate the link variables and all relevant vectors for the inner CG loop. After the completion of the inner CG loop and the vector S (12) is computed, the

memory space of $2n + 3$ column vectors is released, and the vectors $\{Y_\sigma\}$ and $\{P_\sigma\}$ of the outer CG loop can be read from the hard disk, which are then updated to new values according to the CG algorithm.

With this simple scheme of memory management, the minimal memory for computing one of the 12 columns of the quark propagators (for a set of bare quark masses) on the $16^3 \times 32$ lattice with $n = 16$ (degree of Zolotarev rational polynomial) becomes

$$N_{cg}^{min} \times N_v = 38 \times 0.024 = 0.912 \text{ Gbyte.}$$

Thus the computation can be performed at a single node with one Gbyte of memory, which can be implemented by installing four stripes of 256 Mbyte memory modules, a much more economic solution than using 4×512 Mbyte modules. Moreover, the time for disk I/O (at the interface of inner and outer CG loops) only constitutes a few percent of the total time for the execution of the entire nested CG loops (Table 3). This is the optimal memory configuration for a PC cluster to compute quark propagators on the $16^3 \times 32$ lattice, which of course is not necessarily the optimal one for other lattice sizes. However, our simple scheme of memory management for the nested CG loops should be applicable to any lattice sizes, as well as to other systems.

In passing, we emphasize that the Zolotarev optimal rational approximation to $(H_w^2)^{-1/2}$ plays a crucial role to minimize the number of vectors required for the inner CG loop. If one had used other rational approximations, then it would require a very large n to preserve exact chiral symmetry to a high precision (e.g., $\sigma < 10^{-11}$). In that case, it would be impossible to attain the optimal price/performance as what has been outlined above.

4 The SSE2 acceleration

With the optimal memory allocation for each node, we further enhance the performance of our lattice QCD codes (in Fortran) by rewriting its computationally intense parts in the SSE2 assembly codes of Pentium 4. In this section, we briefly review the basic features of the vector unit (SSE2) of Pentium 4, and then describe how to implement SSE2 codes in our lattice QCD program.

4.1 The basic features of SSE2

The simplest and the most efficient scheme of parallel computation is Single Instruction Multiple Data (SIMD). It can be implemented inside CPU through a set of long registers. If each register can accommodate several (say, s) data entries, then any operation (addition, subtraction, multiplication and division) on these registers will act on all data entries in parallel, thus yields the speed-up by a factor of s comparing with normal registers. A schematic diagram is shown in Fig. 2.

Even though Intel had implemented the vector unit in their CPUs since Pentium-MMX series, only in the most recent IA-32 Pentium 4 and the advanced IA-64 Itanium, the architecture has been extended to SSE2 (Streamed SIMD Extension 2) to incorporate double precision data entries.

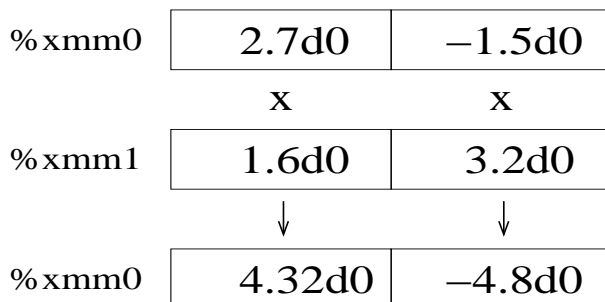


Figure 2: Double precision multiplication performed by the SSE2 instruction in the SIMD registers.

The Pentium 4 processor has eight registers (%xmm0, %xmm1, ..., %xmm7) for SIMD operations [18]. Each register is 128 bits wide and can accommodate 4 integers, or 4 single-precision or 2 double-precision floating point numbers. Since we always use double precision floating point numbers in our program, the execution speed of our program can be almost doubled if SSE2 is turned on judiciously in the computationally intensive parts. Note that SSE2 complies with the IEEE 32-bit and 64-bit arithmetic, thus the precision is lower than the extended 80-bit precision of the normal registers in Pentium 4. However, the difference is less than one part in 10^{15} (double precision), thus is negligible in our computations.

4.2 How to implement SSE2 codes in Fortran programs

Since our lattice QCD codes were originally written in Fortran 77, it would be natural if SSE2 codes can be directly embedded in our Fortran program. However, to our knowledge, the Fortran compilers currently available in the market do not support the option of inlining SSE2 codes. Moreover, for optimal performance of SSE2, the data should be aligned to 16-byte memory boundary. This can be easily carried out in C. Therefore our strategy to implement SSE2 codes is rewrite the main program unit in C such that the data arrays are allocated and aligned to 16 bytes memory boundary, then the SSE2 codes are embedded in C subroutines which are then called by original routines in Fortran.

Of course, if one has written lattice QCD codes in C, then the SSE2 codes can be embedded in C routines directly, without dealing with the interface of C and Fortran.

In the following, we illustrate our scheme of implementing SSE2 codes with an example program. The default compilers are `gcc` and `g77` in Linux.

```

program main
  implicit none
  integer n
  parameter (n=100)
  double precision r(n), v(n)
  call vxzero(n, r, v)
end

subroutine vxzero(n, r, v)
  implicit none

```

```

integer n
double precision c, r(*), v(*)
...
call vadd(n, c, r, v)           ! r = r + c v
...                             ! c:   scalar
end                             ! r, v: vector

```

Here the Fortran **main** program calls the subroutine **vxzero** which in turn calls a computationally intensive routine **vadd**.

First, we rewrite the main program in C, with the data arrays allocated and properly aligned.

```

#include <malloc.h>
int main(int argc, char **argv)
{
    int n=100;
    double *r, *v;
    /* setup the environment for Fortran */
    f_setarg(argc, argv);
    f_setsig();
    f_init();
    /* allocate r & v, and align them to 16-byte boundary */
    r = memalign(16, n*sizeof(double));
    v = memalign(16, n*sizeof(double));
    /* call the Fortran subroutine */
    vxzero_(&n, r, v);
    /* shutdown the I/O channels of Fortran */
    f_exit();
    exit(0);
    return 0;
}

```

The function call **memalign()** dynamically allocates 16 bytes aligned pointers **r** and **v**. Then the aligned arrays **v[]** and **r[]** can be passed to C subroutines for SSE2 operations.

Next we rewrite the computationally intensive routine **vadd** in C with embedded SSE2 codes.

```

/* load variable a into %%xmm0 */
#define sse_load(a) \
    __asm__ __volatile__ ( "movapd %0, %%xmm0" :: "m" (a))

/* r = r + %%xmm0 x v */
#define sse_add(r, v) \
    __asm__ __volatile__ ( \
        "movapd %1, %%xmm1 \n\t" \

```

```

        "movapd %2, %%xmm2 \n\t"    \
        "mulpd %%xmm0, %%xmm2 \n\t" \
        "addpd %%xmm1, %%xmm2 \n\t" \
        "movapd %%xmm2, %0"        \
        :                            \
/* store to address (r), which is indexed as %0 */ \
    "=m" (r)                          \
    :                                    \
/* load from address (r) and (v), which are \
   indexed as %1 and %2, respectively */ \
    "m" (r), "m" (v))

#define ALIGN16 __attribute__((aligned (16)))

void vadd_(int *n, double *coeff, double *r, double *v)
{
    int i, len;
    static double cc[2] ALIGN16;

/* the array cc is aligned to 16-byte boundary */

    cc[0] = cc[1] = *coeff;
    sse_load(cc[0]);
    len = (*n)/2;
    for (i=0; i<len*2; i+=2) {
        sse_add(r[i], v[i]);
    }
    if (*n % 2 != 0)
        r[len*2] = r[len*2] + cc[0] * v[len*2];
}

```

Note that we have added the keyword `__volatile__` (an GNU extension) in the macro `__asm__`. Its purpose is to ensure that the compiler does not rearrange the order of execution of the codes during compilation. Finally, all object modules are linked by `gcc` with the option `-lg2c`.

4.3 The implementation of H_w times $|v\rangle$

In our lattice QCD program, most of the execution time is spent in solving quark propagators via the nested CG loops. Thus the execution time is dominated by the operation H_w times $|v\rangle$, which is performed many times ($> 10^5$ in most cases) before the final results of quark propagators can be obtained. Thus it is crucial to optimize this operation with SSE2 codes.

First, we have to set up the correspondence between the data structures used by C and Fortran routines in our program, in particular, for the link variables and the relevant vectors in the nested CG loops.

Suppose we write the arrays of link variables and a column vector v in the syntax of Fortran as

$$u(i, j, \mu, x),$$

$$v(i, k, x),$$

where i and j are the color indices, μ is the space-time direction, k is the spinor index, and x is the site index. Now the question is how to access the elements of these arrays in C routines. To resolve this problem, we define some data structures in C as follows.

```

/* SU(3) matrix, (c01,c02) forms the complex number of u11, and
(c03,c04) of u21, etc. */
typedef struct {
    double c01, c02, c03, c04, c05, c06;
    double c07, c08, c09, c10, c11, c12;
    double c13, c14, c15, c16, c17, c18;
} su3_t;

/* there are 4 link variables at each site. */
typedef struct {
    su3_t mu1, mu2, mu3, mu4;
} ulink_t;

/* SU(3) vector, (c1,c2) forms the complex number of v1,
(c3,c4) of v2, and (c5,c6) of v3. */
typedef struct {
    double c1, c2, c3, c4, c5, c6;
} vector_t;

/* SU(3) Dirac spinor. */
typedef struct {
    vector_t s1, s2, s3, s4;
} spinor_t;

```

Then the correspondence can be easily established. For example, the elements $u(3, 2, 1, x)$ and $v(2, 4, x)$ can be accessed by C routines as $(u[x].mu1.c11, u[x].mu1.c12)$ and $(v[x].s4.c3, v[x].s4.c4)$ respectively.

Now we rewrite H_w as

$$H_w(x, y) = \gamma_5 \left\{ (4 - m_0)\delta_{x,y} + \frac{1}{2} \sum_{\mu=1}^4 [(-1 + \gamma_\mu)U_\mu(x)\delta_{x+\mu,y} - (1 + \gamma_\mu)U_\mu^\dagger(x - \mu)\delta_{x-\mu,y}] \right\}$$

Then the multiplication of H_w to a column vector $|v\rangle$ can be optimized by minimizing the number of multiplications involving the link variables. For example, the multiplication in $(-1 + \gamma_1)u|v\rangle$ can be written as (in the spinor space)

$$(-\mathbb{1} + \gamma_1)u|v\rangle = \begin{pmatrix} r_1 \\ r_2 \\ r_3 \\ r_4 \end{pmatrix} = \begin{pmatrix} -u & 0 & 0 & u \\ 0 & -u & u & 0 \\ 0 & u & -u & 0 \\ u & 0 & 0 & -u \end{pmatrix} \begin{pmatrix} v_1 \\ v_2 \\ v_3 \\ v_4 \end{pmatrix} = \begin{pmatrix} u(v_4 - v_1) \\ u(v_3 - v_2) \\ -r_2 \\ -r_1 \end{pmatrix}$$

where all indices are suppressed except the spinor indices. It is clear that the vectors $v_4 - v_1$ and $v_3 - v_2$ should be computed first, before they are multiplied by link variable u (generic symbol for $U_\mu/2$). For example, the operation $v_4 - v_1$ can be performed by the following macros with SSE2.

```
#define mvpv(v1, v2) \
    __asm__ __volatile__ ( \
        "movapd %0, %%xmm0 \n\t" \
        "movapd %1, %%xmm1 \n\t" \
        "movapd %2, %%xmm2 \n\t" \
        "subpd %3, %%xmm0 \n\t" \
        "subpd %4, %%xmm1 \n\t" \
        "subpd %5, %%xmm2" \
        : : \
        "m" ((v2).c1), \
        "m" ((v2).c3), \
        "m" ((v2).c5), \
        "m" ((v1).c1), \
        "m" ((v1).c3), \
        "m" ((v1).c5))
```

Similarly, we have

$$\begin{aligned}
(-\mathbb{1} - \gamma_1)u^\dagger |v\rangle &= \begin{pmatrix} r_1 \\ r_2 \\ r_3 \\ r_4 \end{pmatrix} = \begin{pmatrix} -u^\dagger(v_4 + v_1) \\ -u^\dagger(v_3 + v_2) \\ r_2 \\ r_1 \end{pmatrix}, \\
(-\mathbb{1} + \gamma_2)u |v\rangle &= \begin{pmatrix} r_1 \\ r_2 \\ r_3 \\ r_4 \end{pmatrix} = \begin{pmatrix} -u(v_1 + iv_4) \\ -ir_3 \\ -u(v_3 + iv_2) \\ -ir_1 \end{pmatrix}, \\
(-\mathbb{1} - \gamma_2)u^\dagger |v\rangle &= \begin{pmatrix} r_1 \\ r_2 \\ r_3 \\ r_4 \end{pmatrix} = \begin{pmatrix} -ir_4 \\ -u^\dagger(v_2 + iv_3) \\ -ir_2 \\ -u^\dagger(v_4 + iv_1) \end{pmatrix}, \\
(-\mathbb{1} + \gamma_3)u |v\rangle &= \begin{pmatrix} r_1 \\ r_2 \\ r_3 \\ r_4 \end{pmatrix} = \begin{pmatrix} u(v_3 - v_1) \\ -u(v_2 + v_4) \\ -r_1 \\ r_2 \end{pmatrix}, \\
(-\mathbb{1} - \gamma_3)u^\dagger |v\rangle &= \begin{pmatrix} r_1 \\ r_2 \\ r_3 \\ r_4 \end{pmatrix} = \begin{pmatrix} -u^\dagger(v_1 + v_3) \\ u^\dagger(v_4 - v_2) \\ r_1 \\ -r_2 \end{pmatrix},
\end{aligned}$$

$$\begin{aligned}
(-\mathbb{1} + \gamma_4)u|v\rangle &= \begin{pmatrix} r_1 \\ r_2 \\ r_3 \\ r_4 \end{pmatrix} = \begin{pmatrix} -ir_3 \\ -ir_4 \\ -u(v_3 + iv_1) \\ -u(v_4 + iv_2) \end{pmatrix}, \\
(-\mathbb{1} - \gamma_4)u^\dagger|v\rangle &= \begin{pmatrix} r_1 \\ r_2 \\ r_3 \\ r_4 \end{pmatrix} = \begin{pmatrix} -u^\dagger(v_1 + iv_3) \\ -u^\dagger(v_2 + iv_4) \\ -ir_1 \\ -ir_2 \end{pmatrix}.
\end{aligned}$$

So the multiplications involving the link variables can be implemented as

```

/* for each lattice size */
for (x=0; x<ldim; x++) {
/* prefetch for the current multiplication */
  y = iup[x].mu1-1;
  _prefetch_su3(&(u[x].mu1));
  _prefetch_spinor(&(v[y]));
/* prefetch for the next multiplication */
  z = idn[x].mu1-1;
  _prefetch_su3(&(u[z].mu1));
  _prefetch_spinor(&(v[z]));
/* r1.s1 = u[x].mu1 * (v[y].s4 - v[y].s1) */
  mvpv(v[y].s1, v[y].s4);
  su3mul(r1.s1, u[x].mu1);
/* r1.s2 = u[x].mu1 * (v[y].s3 - v[y].s2) */
  mvpv(v[y].s2, v[y].s3);
  su3mul(r1.s2, u[x].mu1);
/* r1.s3 = -r1.s2 */
  mvset(r1.s3, r1.s2);
/* r1.s4 = -r1.s1 */
  mvset(r1.s4, r1.s1);

/* prefetch for the next multiplication */
  y = iup[x].mu2-1;
  _prefetch_su3(&(u[x].mu2));
  _prefetch_spinor(&(v[y]));
/* r2.s1 = -(u[x].mu1)^\dagger * (v[y].s1 + v[y].s4) */
  mvmv(v[z].s1, v[z].s4);
  su3Hmul(r2.s1, u[z].mu1);
/* r2.s2 = -(u[x].mu1)^\dagger * (v[y].s2 + v[y].s3) */
  mvmv(v[z].s2, v[z].s3);
  su3Hmul(r2.s2, u[z].mu1);
/* r2.s3 = r2.s2 */
  pvset(r2.s3, r2.s2);
/* r2.s4 = r2.s1 */
  pvset(r2.s4, r2.s1);

```

...

where $\mathbf{r1}$, $\mathbf{r2}$, ..., and $\mathbf{v}[]$ are declared as the type `spinor_t`, and $\mathbf{u}[]$ is declared as the type `ulink_t`. Note that prefetching has been inserted in order to attain the optimal performance. Finally, we have 8 vector segments $\mathbf{r1}$, ..., $\mathbf{r8}$, and a diagonal term. They are summed over to give the final result of $v[y]$,

$$\begin{aligned}
v[y].s1 &= r1.s1 + r2.s1 + r3.s1 + r4.s1 + r5.s1 + r6.s1 + r7.s1 + r8.s1 \\
&\quad + (4 - m_0) * v[x].s1, \\
v[y].s2 &= r1.s2 + r2.s2 + r3.s2 + r4.s2 + r5.s2 + r6.s2 + r7.s2 + r8.s2 \\
&\quad + (4 - m_0) * v[x].s2, \\
v[y].s3 &= -(r1.s3 + r2.s3 + r3.s3 + r4.s3 + r5.s3 + r6.s3 + r7.s3 + r8.s3) \\
&\quad + (4 - m_0) * v[x].s3, \\
v[y].s4 &= -(r1.s4 + r2.s4 + r3.s4 + r4.s4 + r5.s4 + r6.s4 + r7.s4 + r8.s4) \\
&\quad + (4 - m_0) * v[x].s4,
\end{aligned}$$

Next we come to the question how to implement SSE2 codes for a $SU(3)$ matrix times a vector, the most crucial part in H_w times $|v\rangle$. This problem has been solved by Lüscher [19], and his SSE2 codes is available in the public domain [20]. We found that Lüscher's code is quite efficient, and have adopted it in our program. For completeness, we briefly outline Lüscher's algorithm as follows.

Consider

$$\begin{pmatrix} u_{11} & u_{12} & u_{13} \\ u_{21} & u_{22} & u_{23} \\ u_{31} & u_{32} & u_{33} \end{pmatrix} \times \begin{pmatrix} y_1 \\ y_2 \\ y_3 \end{pmatrix} = \begin{pmatrix} r_1 \\ r_2 \\ r_3 \end{pmatrix}$$

First, the elements (y_1, y_2, y_3) of the vector $|y\rangle$ are copied to the registers `%xmm0`, `%xmm1`, and `%xmm2`, respectively. Then the real part of the $SU(3)$ matrix $\{u_{mn}\}$ is read sequentially, and is multiplied to $|y\rangle$ at `%xmm0`, `%xmm1`, and `%xmm2`, and the result is stored at `%xmm3`, `%xmm4`, and `%xmm5`,

$$\begin{aligned}
\%xmm0 &= (\text{Re}(y_1), \text{Im}(y_1)), \\
\%xmm1 &= (\text{Re}(y_2), \text{Im}(y_2)), \\
\%xmm2 &= (\text{Re}(y_3), \text{Im}(y_3)), \\
\%xmm3 &= (t_1, t_2), \\
\%xmm4 &= (t_3, t_4), \\
\%xmm5 &= (t_5, t_6),
\end{aligned}$$

where

$$\begin{aligned}
t_1 &= \text{Re}(u_{11})\text{Re}(y_1) + \text{Re}(u_{12})\text{Re}(y_2) + \text{Re}(u_{13})\text{Re}(y_3), \\
t_2 &= \text{Re}(u_{11})\text{Im}(y_1) + \text{Re}(u_{12})\text{Im}(y_2) + \text{Re}(u_{13})\text{Im}(y_3), \\
t_3 &= \text{Re}(u_{21})\text{Re}(y_1) + \text{Re}(u_{22})\text{Re}(y_2) + \text{Re}(u_{23})\text{Re}(y_3), \\
t_4 &= \text{Re}(u_{21})\text{Im}(y_1) + \text{Re}(u_{22})\text{Im}(y_2) + \text{Re}(u_{23})\text{Im}(y_3), \\
t_5 &= \text{Re}(u_{31})\text{Re}(y_1) + \text{Re}(u_{32})\text{Re}(y_2) + \text{Re}(u_{33})\text{Re}(y_3), \\
t_6 &= \text{Re}(u_{31})\text{Im}(y_1) + \text{Re}(u_{32})\text{Im}(y_2) + \text{Re}(u_{33})\text{Im}(y_3).
\end{aligned}$$

Lattice Size	SSE2 off	SSE2 on	speed-up
$8^3 \times 24$	0.034	0.018	1.89
$10^3 \times 24$	0.065	0.036	1.81
$12^3 \times 24$	0.110	0.063	1.75
$16^3 \times 32$	0.328	0.183	1.79

Table 1: The execution time (in unit of second) for H_w multiplying a column vector Y , with SSE2 turned on and off. The test is performed at a Pentium 4 (2 GHz) node.

Next, multiply the vector y by $i = (0, 1)$, i.e.,

$$\begin{aligned}
\%xmm0 &\rightarrow (\text{Im}(y_1), \text{Re}(y_1)) \rightarrow (-\text{Im}(y_1), \text{Re}(y_1)), \\
\%xmm1 &\rightarrow (\text{Im}(y_2), \text{Re}(y_2)) \rightarrow (-\text{Im}(y_2), \text{Re}(y_2)), \\
\%xmm2 &\rightarrow (\text{Im}(y_3), \text{Re}(y_3)) \rightarrow (-\text{Im}(y_3), \text{Re}(y_3)),
\end{aligned}$$

which is implemented by the following SSE2 code

```

static int sn3[4] ALIGN16 = {0x0,0x80000000,0x0,0x0};
#define su3mul(r, u) \
    ... \
    "xorpd %9, %%xmm0 \n\t" \
    "xorpd %9, %%xmm1 \n\t" \
    "xorpd %9, %%xmm2 \n\t" \
    ... \
    :: \
    ... \
    "m" (sn3[0]);

```

Then the imaginary part of $\{u_{mn}\}$ is read and multiplied to iy , and the final result is

$$\begin{aligned}
\%xmm3 &= (t_1 + s_1, t_2 + s_2), \\
\%xmm4 &= (t_3 + s_3, t_4 + s_4), \\
\%xmm5 &= (t_5 + s_5, t_6 + s_6),
\end{aligned}$$

where

$$\begin{aligned}
s_1 &= -\text{Im}(u_{11})\text{Im}(y_1) - \text{Im}(u_{12})\text{Im}(y_2) - \text{Im}(u_{13})\text{Im}(y_3), \\
s_2 &= +\text{Im}(u_{11})\text{Re}(y_1) + \text{Im}(u_{12})\text{Re}(y_2) + \text{Im}(u_{13})\text{Re}(y_3), \\
s_3 &= -\text{Im}(u_{21})\text{Im}(y_1) - \text{Im}(u_{22})\text{Im}(y_2) - \text{Im}(u_{23})\text{Im}(y_3), \\
s_4 &= +\text{Im}(u_{21})\text{Re}(y_1) + \text{Im}(u_{22})\text{Re}(y_2) + \text{Im}(u_{23})\text{Re}(y_3), \\
s_5 &= -\text{Im}(u_{31})\text{Im}(y_1) - \text{Im}(u_{32})\text{Im}(y_2) - \text{Im}(u_{33})\text{Im}(y_3), \\
s_6 &= +\text{Im}(u_{31})\text{Re}(y_1) + \text{Im}(u_{32})\text{Re}(y_2) + \text{Im}(u_{33})\text{Re}(y_3).
\end{aligned}$$

Arnoldi vectors	Iterations	Time
40	756	12923
50	160	4757
60	108	4730
70	82	4414
80	65	4131
90	55	4103
100	46	4100
120	37	4251
140	32	4869
160	26	5002

Table 2: The execution time (in unit of second) for projecting 20 low-lying eigenmodes of H_w^2 using ARPACK, versus the number of Arnoldi vectors. The test is performed at a Pentium 4 (1.6 GHz) node, for a gauge configuration on the $8^3 \times 24$ lattice, at $\beta = 5.8$. Each eigenmode satisfies $\|(H_w^2 - \lambda^2)|x\rangle\| < 10^{-13}$.

5 Performance of the system

In this section, we measure the performance of our system by a number of tests pertaining to the computation of quark propagators.

In Table 1, we list the execution time (in unit of second) for H_w multiplying a column vector Y , for both cases with SSE2 turned on and off, and for several lattice sizes. The data shows that turning on SSE2 can speed up our program by a factor ~ 1.8 .

In Table 2, we list the execution time (in unit of second) for projecting 20 low-lying eigenmodes of H_w^2 using ARPACK, versus the number of Arnoldi vectors. It is clear that there exists an optimal number of Arnoldi vectors for a projection, which of course depends on the gauge configuration. In Table 2, the optimal number is ~ 100 , which amounts to ~ 240 Mbyte for the $8^3 \times 24$ lattice. However, for larger lattices such as $16^3 \times 32$, the optimal number may require more than one gigabyte of memory. In this case, the projection of eigenmodes is carried out at some nodes with 2 gigabyte of memory.

In Table 3, we measure the time used by disk I/O in our simple scheme of memory management for the nested CG loops, versus the number of bare quark masses. The test is performed at a Pentium 4 (2 GHz) node, for the $16^3 \times 32$ lattice, and with 16 projected eigenmodes. The disk I/O time is the difference of the total execution time between two cases of turning on and off of the memory management. It is remarkable that the percentage of disk I/O time is only 3% of the total execution time even for 16 bare quark masses, and with 16 projected eigenmodes. Evidently, for the $16^3 \times 32$ lattice, our simple scheme of memory management is more efficient and less expensive than any other options, e.g., parallel computing (with MPI) through a fast network switch.

In Table 4, we list the execution time (in unit of second) for a Pentium 4 (2 GHz) node to compute 12 columns of quark propagators in a topologically nontrivial gauge background at $\beta = 5.8$ on the $8^3 \times 24$ lattice, versus the number of projected low-lying eigenmodes. Other parameters for the test are: the degree of Zolotarev rational polynomial is $n = 16$; the number

N_m	1	8	16
CG time	491.9	494.8	497.1
disk I/O time	7.6	8.9	14.3
Total time	499.5	503.7	511.4
disk I/O (%)	1.5%	1.8%	2.9%

Table 3: The percentage of time spent in memory management (disk I/O) versus the number of bare quark masses (N_m). The test is performed at a Pentium 4 (2 GHz) node, for the $16^3 \times 32$ lattice, and with 16 projected eigenmodes. The time (in unit of second) shown here is only for completing one outer CG iteration for one column of D^{-1} .

of bare quark masses is $N_m = 12$; each projected eigenmode satisfies $\|(H_w^2 - \lambda^2)|x\rangle\| < 10^{-13}$, and the stopping criterion for inner and outer CG loops is $\epsilon = 10^{-11}$. The execution time is decomposed into three parts : (i) the projections of high and low-lying eigenmodes⁴; (ii) computing 12 columns of $(DD^\dagger)^{-1}$ via the nested CG loops; and (iii) computing D^\dagger and multiplying it to $(DD^\dagger)^{-1}$. The total time is listed in the last column of the table. For completeness, we also list λ_{max} and λ_{min} of $|\bar{H}_w|$ (after the projections), the total numbers of iterations of the outer CG loop and average iterations of the inner CG loop, as well as the precision of exact chiral symmetry in terms of σ (13). Evidently, the time for projecting out the high and low-lying eigenmodes is only a very small fraction of the total execution time for computing 12 columns of quark propagators. However, the projections have very significant impacts on the total execution time since it yields the speed-up by a factor of 2.44, as comparing the first row (no projections) with the last row (projections of 40 low-lying eigenmodes). Moreover, with projections, the exact chiral symmetry can be easily preserved to a very high precision ($\sigma < 10^{-13}$). This suggests that *one should project as many low-lying eigenmodes as possible*, before executing the nested CG loops. In general, we suspect that the optimal number of projections depends on the projection algorithm, the amount of memory of the system, as well as the gauge configuration.

In Table 5, we measure the precision of exact chiral symmetry σ (13) versus the degree (n) of Zolotarev optimal rational polynomial. The values of σ listed in the second column of Table 5 are the maxima in the nested CG loops. The execution time and the iterations of the nested CG loops are also listed. Evidently, the precision of exact chiral symmetry σ is quite different from the stopping criterion $\epsilon = 10^{-11}$ for inner and outer CG loops, since σ can be much bigger or smaller than ϵ , as shown in Table 5, as well as in Tables 4 and 6. It is clear that the necessary condition for preserving exact chiral symmetry to a very high precision is to use a higher degree (n) Zolotarev rational polynomial for $(H_w^2)^{-1/2}$. In Ref. [13], tables are provided for looking up which degree n is required to attain one's desired accuracy in preserving the exact chiral symmetry on the lattice, versus the parameter $b = \lambda_{max}^2/\lambda_{min}^2$ of a given gauge configuration.

In Table 6, we list the execution time (in unit of second) of a Pentium 4 (2 GHz) node to compute 12 columns of quark propagators, versus the size of the lattice. The parameters for the test are: the degree of Zolotarev rational polynomial is $n = 16$, the number of bare quark

⁴Note that the projection time listed in the 2nd column of Table 4 includes 167 seconds for projecting 4 highest eigenmodes of H_w^2 .

projections		λ_{min}	λ_{max}	inner CG		outer CG		χ sym.	CG	D^\dagger mult.	Total
#	time			ave. iters.	tot. iters.	$\sigma(\text{max.})$	time	time	time		
0	0	0.017	6.207	965	1282	4.5×10^{-10}	137221	15070	152291		
8	1573	0.138	6.207	552	1282	5.2×10^{-14}	70908	7828	80309		
16	2753	0.165	6.207	475	1282	5.7×10^{-14}	61543	6803	71099		
24	3703	0.178	6.207	443	1282	4.3×10^{-14}	57792	6374	67869		
32	4725	0.198	6.207	403	1282	5.3×10^{-14}	52961	5864	63550		
40	6524	0.211	6.207	378	1282	6.0×10^{-14}	50301	5581	62406		

Table 4: The execution time for a Pentium 4 (2 GHz) node to compute 12 columns of quark propagators, versus the number of projected low-lying eigenmodes. The parameters for the test are : the lattice size is $8^3 \times 24$; $\beta = 5.8$; the degree of Zolotarev rational polynomial is $n = 16$; the number of bare quark masses is $N_m = 12$ and $ma \geq 0.06$; each projected eigenmode satisfies $\|(H_w^2 - \lambda^2)|x\rangle\| < 10^{-13}$; and the stopping criterion for inner and outer CG loops is $\epsilon = 10^{-11}$.

Zolo. degree	χ sym. $\sigma(\text{max.})$	CG iters.		CG time	D^\dagger mult. time	Total time
4	1.7×10^{-4}	367	286	82393	4493	86885
8	1.5×10^{-8}	402	288	111247	6003	117250
10	2.9×10^{-10}	408	288	120940	6520	127460
12	6.4×10^{-12}	411	288	129188	6962	136150
16	1.4×10^{-13}	414	288	148654	8006	156660

Table 5: The precision of exact chiral symmetry σ versus the degree (n) of the Zolotarev rational polynomial. The test is performed at a Pentium 4 (2 GHz) node, with the parameters: lattice size= $16^3 \times 32$; $\beta = 6.0$; the number of bare quark masses is $N_m = 16$; the number of projected eigenmodes is $k = 20$; each projected eigenmode satisfies $\|(H_w^2 - \lambda^2)|x\rangle\| < 10^{-13}$; $b = \lambda_{max}^2/\lambda_{min}^2 = 1086$; and the stopping criterion for the CG loops is $\epsilon = 10^{-11}$.

masses is $N_m = 16$ and $ma \geq 0.02$, each projected eigenmode satisfies $\|(H_w^2 - \lambda^2)|x\rangle\| < 10^{-13}$, and the stopping criterion for the inner and the outer CG loops is $\epsilon = 10^{-11}$. From the last entry of the last row, we can estimate that a Pentium 4 (2 GHz) node takes about 24 days to complete 12 columns of quark propagators (for 16 bare quark masses) for one gauge configuration at $\beta = 6.0$ on the $16^3 \times 32$ lattice. In other words, if we have 12 nodes and let each one of them work on one column of D^{-1} , then we can complete the quark propagators for one gauge configuration in two days. Since our system consists of 64 nodes, so we can compute quark propagators at a rate more than five gauge configurations per two days.

6 Conclusions

In this paper, we outline the essential features of a Linux PC cluster (64 nodes) which has been built at National Taiwan University, and discuss how to optimize its hardware and software for lattice QCD with exact chiral symmetry. At present, all nodes are working around the clock on lattice QCD computations.

With Zolotarev optimal rational approximation to $(H_w^2)^{-1/2}$, projections of high and low-lying eigenmodes of H_w^2 , the multi-mass CG algorithm, the SSE2 acceleration, and our simple scheme of memory management, we are able to compute quark propagators of 16 bare quark masses on the $16^3 \times 32$ lattice, with the precision of quark propagators up to 10^{-11} and the precision of exact chiral symmetry up to 10^{-12} , at the rate of 2.5 gauge configuration ($\beta = 6.0$) per day, with our present system of 64 nodes. This demonstrates that an optimized Linux PC cluster can be a viable computational system to extract physical quantities from lattice QCD with exact chiral symmetry [9, 21, 22].

The speed of our system is higher than 70 Gflops, and the total cost of the hardware is less than US\$60000. This amounts to price/performance ratio better than \$1.0/Mflops for 64-bit (double precision) computations. The basic idea of optimization is to let each node work independently on one of the 12 columns of the quark propagators (for a set of bare quark masses), and also use the hard disk as the virtual memory for the vectors in the outer CG loop, while the CPU is working on the inner CG loop. Our simple scheme of memory management for the nested CG loops may also be useful to other systems.

In future, we will add more nodes to our system, and will also work on larger lattices, say $24^3 \times 48$. Then one Gbyte memory at each node is not sufficient to accommodate all relevant vectors in the inner CG loop, even for 12 Zolotarev terms. However, there are several ways to circumvent this problem. First, our memory management scheme is quite versatile, which is more than just for swapping the vectors at the interface of inner and outer CG loops. In fact, it can handle any number of Zolotarev terms for any lattice size, and can automatically minimize disk I/O at any step of the nested CG loops, according to the amount of physical memory of a node. As long as the percentage of the disk I/O time is less than 30%, it is still a better option than distributing the nested CG loops across the nodes and performing parallel computations (with MPI) through a fast network switch, since the communication overheads is expected to be more than 30% of the total time, especially for a system of 100 nodes or more. Secondly, we can increase the amount of memory at each node, which depends on the specification of the motherboard as well as the price and the capacity of the memory modules. Finally, we can also exploit algorithms [23] which only use five vectors rather than $2n + 3$ vectors for the inner CG loop, or the Lanczos algorithm as described in Ref. [24]. Now

Lattice	projections			λ_{min}	λ_{max}	χ sym $\sigma(\text{max.})$	inner CG ave. iters.	outer CG tot. iters.	CG time	D^\dagger mult. time	disk I/O time	Total time
	β	#	time									
$8^3 \times 24$	5.8	32	4725	0.198	6.207	5.4×10^{-14}	403	1322	54384	7804	0	66913
$10^3 \times 24$	5.8	30	7803	0.152	6.204	6.4×10^{-14}	519	1943	191861	18626	0	218290
$12^3 \times 24$	5.8	30	13258	0.129	6.211	9.8×10^{-14}	608	2840	574226	38234	0	625718
$16^3 \times 32$	6.0	20	74937	0.215	6.260	3.3×10^{-13}	370	3968	1866172	87890	66976	2095975

Table 6: The execution time (in unit of second) of a Pentium 4 (2 GHz) node to compute 12 columns of quark propagators, versus the size of the lattice. The parameters for the test are: the degree of Zolotarev rational polynomial is $n = 16$, the number of bare quark masses is $N_m = 16$ and $ma \geq 0.02$, the precision of each projected eigenmode satisfies $\|(H_w^2 - \lambda^2)|x\rangle\| < 10^{-13}$, and the stopping criterion for inner and outer CG loops is $\epsilon = 10^{-11}$.

it is clear that a Linux PC cluster is a viable platform to tackle lattice QCD with exact chiral symmetry even for a large lattice (e.g., $32^3 \times 64$), though more studies are needed before one reaches an optimal design for dynamical quarks.

Note added in proof:

Recently, it has been shown [25] that the speed of Neuberger's double pass algorithm [23] for computing the matrix-vector product $R^{(n-1,n)}(H_w^2) \cdot Y$ is almost independent of the degree n of the rational polynomial, and it is faster than the single pass for $n > 13$ (for Pentium 4 with SSE2). Thus the single pass has been replaced with the double pass algorithm in our Linux PC cluster.

Acknowledgement

This work was supported in part by the National Science Council, ROC, under the grant number NSC90-2112-M002-021.

References

- [1] T. W. Chiu, “A Parallel Computer For Lattice Gauge Theories,” Proceedings of the Third Conference on Hypercube Concurrent Computers and Applications, edited by G.C. Fox, published by ACM, New York, N.Y.(1988) p. 81-91.
- [2] D. B. Kaplan, Phys. Lett. B **288**, 342 (1992)
- [3] H. Neuberger, Phys. Lett. B **417**, 141 (1998); R. Narayanan and H. Neuberger, Nucl. Phys. B **443**, 305 (1995)
- [4] M. Creutz, Phys. Rev. D **21** (1980) 2308.
- [5] N. Cabibbo and E. Marinari, Phys. Lett. B **119** (1982) 387.
- [6] T. W. Chiu, Phys. Rev. D **60**, 034503 (1999)
- [7] P. H. Ginsparg and K. G. Wilson, Phys. Rev. D **25**, 2649 (1982).
- [8] T. W. Chiu and S. V. Zenkin, Phys. Rev. D **59**, 074501 (1999)
- [9] T. W. Chiu and T. H. Hsieh, Phys. Rev. D **66**, 014506 (2002).
- [10] E. I. Zolotarev, “Application of elliptic functions to the questions of functions deviating least and most from zero”, Zap. Imp. Akad. Nauk. St. Petersburg, 30 (1877), no. 5; reprinted in his Collected works, Vol. 2, Izdat, Akad. Nauk SSSR, Moscow, 1932, p. 1-59.
- [11] N. I. Akhiezer, *Theory of approximation*, Reprint of 1956 English translation (Dover, New York, 1992); *Elements of the theory of elliptic functions*, Translations of Mathematical Monographs, 79 (American Mathematical Society, Providence, R.I. 1990)
- [12] J. van den Eshof, A. Frommer, T. Lippert, K. Schilling and H. A. van der Vorst, Nucl. Phys. Proc. Suppl. **106**, 1070 (2002)
- [13] T. W. Chiu, T. H. Hsieh, C. H. Huang and T. R. Huang, Phys. Rev. D **66**, 114502 (2002)
- [14] A. Frommer, B. Nockel, S. Gusken, T. Lippert and K. Schilling, Int. J. Mod. Phys. C **6**, 627 (1995)
- [15] B. Jegerlehner, “Krylov space solvers for shifted linear systems,” hep-lat/9612014.
- [16] R. Lehoucq, D. Sorensen, C. Yang, “ARPACK Users’ Guide: Solution of Large Scale Eigenvalue Problems with Implicitly Restarted Arnoldi Methods”, *Philadelphia: SIAM, 1998*.
- [17] “Intel IA-32 Intel (R) Architecture Software Developer’s Manual”, Volume 1: “Basic Architecture”, Volume 2: “Instruction Set Reference”, <http://www.intel.com/design/pentium4/manuals/>.

- [18] “Intel Floating-Point Arithmetic with Streaming SIMD Extensions and Pentium 4 Processor SSE2 instructions, AP-943”,
ftp://download.intel.com/design/perftool/cbts/appnotes/sse2/w_fp_precision.pdf.
- [19] M. Luscher, Nucl. Phys. Proc. Suppl. **106**, 21 (2002)
- [20] <http://latticeqcd.fnal.gov/software/fermiqcd/index.html>
- [21] T. W. Chiu and T. H. Hsieh, Phys. Lett. B **538**, 298 (2002)
- [22] T. W. Chiu and T. H. Hsieh, Nucl. Phys. Proc. Suppl. **119C**, 793 (2003)
- [23] H. Neuberger, Int. J. Mod. Phys. C **10**, 1051 (1999)
- [24] A. Borici, J. Comput. Phys. **162**, 123 (2000)
- [25] T. W. Chiu and T. H. Hsieh, hep-lat/0306025, Phys. Rev. E (in press).